Space Communications 20 (2005/2006) 69–83
IOS Press

Two approaches for effective modelling of rain-rate time-series for radiocommunication system simulations

C. Alasseur [a], A. Núñez [b], F.P. Fontán [b], L. Husson [a], U.-C. Fiebig [c] and P. Mariño [b]
[a] *Supélec, 3 rue Joliot-Curie, 91192 Gif-sur-Yvette, France*
E-mail: clemence.alasseur@supelec.fr, lionel.husson@supelec.fr
[b] *Universidad de Vigo, ETSE Telecomunicación, Campus Universitario, 36200, Vigo, Spain*
E-mail: fito@tsc.uvigo.es, fpfontan@tsc.uvigo.es, pmarino@uvigo.es
[c] *German Aerospace Center (DLR), Institute for Communications and Navigation, D-82230 Wessling, Germany*
E-mail: Uwe.Fiebig@dlr.de

Abstract. This paper describes two methods for generating synthetic rain rate time-series capable of being used to simulate the performance of radio communication systems operating above 10 GHz. Rain rates are modelled because they are widely available and because an approximate link to signal attenuation can be established owing to the significant correlation between them. The proposed models are based on hierarchic Markov chains. Rain and no rain events are simulated by the outer chain which simulates the rain event duration on the basis of the experimental statistics. The inner chain of both models deals with the rain intensity generation. The models therefore produce simulated rain samples whose statistics very closely match those of the experimental data without using any stored rain time series.

1. Introduction

There is a growing interest in the development of synthetic time-series generators of rain attenuation for satellite propagation channel. Satellite communication systems currently need to operate at higher frequency bands, such as Ka or V bands, owing to congestion at lower bands. At these high frequencies, rain events cause severe attenuation to the propagation channel. To avoid the user experiencing transmission loss, an extra power margin can be used to offset the attenuation caused by rain. However, as rain events do not occur during the major part of the time, this practice leads to inefficient use of resources. Indeed, contrary to terrestrial stations, special care is required for the use of satellite resources owing to their limited capacity. The accurate modelling of rain intensities can be used to counteract rain attenuation efficiently by applying adapted Fade Mitigation Techniques (FMTs). These techniques aim at saving the allocated resources by adapting the transmission to the propagation encountered in real life.

To reflect both the long- and short-term dynamics of rain attenuation, the development of time-series generators has to rely on prolonged experimental observations of attenuation time-series. This is not always feasible, however, especially if all possible climates need to be characterized. Fortunately, for the purposes in hand, rain attenuation is fairly well correlated with rain rate (Fig. 1). Moreover, consistent sets of rain rate time-series are available from numerous observation points around the globe.

This paper presents two methods to model the behaviour of rain time series. Both methods are based on Markov chain structure [1–4]. The first part presents a variation of the second level Markov model presented in [5]. Both levels of this model are Markov chains: the first level generates the time series corresponding to the occurrence, or non-occurrence, of rain events and the second level generates the rain intensity time series when the first level imposes rain event. The global model is shown to produce very accurate rain intensity time series: some commonly used statistics of the simulated data closely match the statistics of the experimental data. A frequentist model validation method is also adopted to test the quality of the proposed model.

The other method, presented in the second part of this paper, is an improvement of the four-state model

presented in [6] and considers two different rain behaviours: the "spiky" and "quasi-flat" events. The two rain type model is therefore comprised by two sub-models, one for each type of rain. Both sub-models include a first and a last rain state for the accurate modelling of the first and last samples of rain events. Tests have been performed to compare synthetically generated rain rate time-series using the new model with real rain rates from an eight-year record taken at Vigo airport on the northwestern coast of Spain. A high degree of similarity has been observed between measured and simulated time-series in terms of first- and, also, second-order statistics.

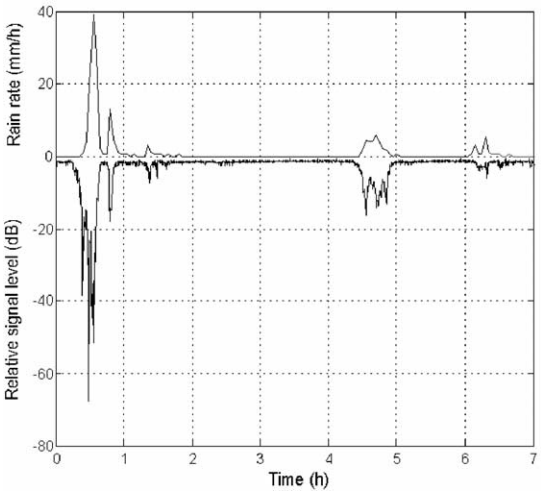

Fig. 1. Measured rain rates and signal levels from Italsat recorded at the DLR site in Wessling near Munich.

It is expected that the proposed models can easily be extended to other locations and climatic zones.

2. First approach: explicit Markov modelled amplitude (EMMA)

The duration of a rain event is not correlated with the distribution of rain and with the Next-Rain Conditional Distribution (NRCD). The NRCD is the distribution of rain samples conditionally onto previous rain samples. Because of this lack of correlation, the global model is then composed of two levels and is represented on Fig. 2. The first level deals with the generation of a rain/inter-rain time series that indicates at any time the occurrence or not of rain events. This first level is a two state Markov chain (rain and inter-rain state) because of the strong underlying Markovian property of the rain/inter-rain indicator. The second level purpose is to generate rain intensities when the first level of the model is in the rain state. A Markov model based on NRCDs is chosen for the second level.

This choice of a Markov model rather than an AR (autoregressive) model is justified by the strong link, on contrary to NRCD, between the correlation of two consecutive rain samples and the rain event duration. It should be noticed that the log of the rain rates are generated and not the direct rain rates.

2.1. 1st level: rain and inter-rain indicator

Inter-rain refers to instants where the rain intensity is null, therefore there are no difficulty to identify rain

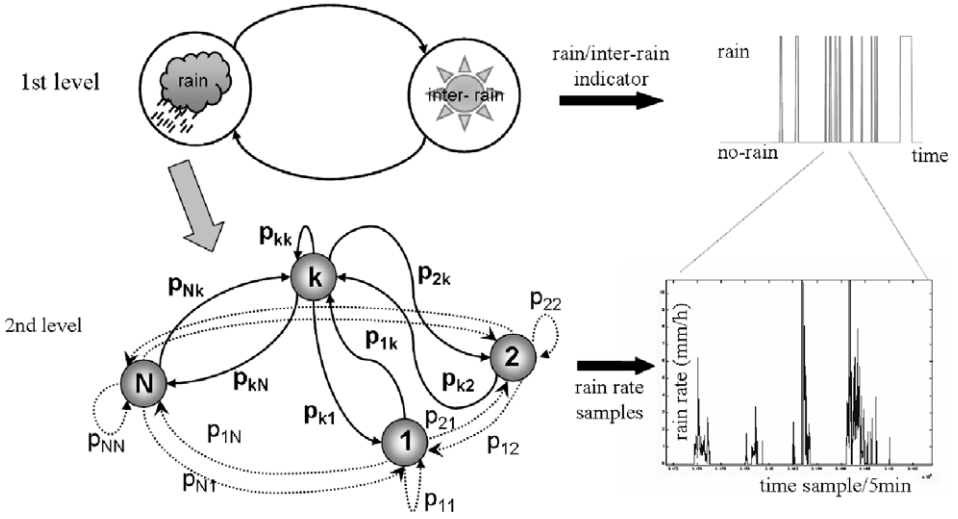

Fig. 2. Global two-level model and corresponding time series.

and inter-rain events. The experimental rain rate time series, used to elaborate the global model, has been measured in Santiago in Spain for a total duration of about 10 years. The time interval between two consecutive samples is roughly 5 minutes and rain rates are measured in mm/h.

Experimental duration distributions of the rain and inter-rain events can not be approximated by an exponential law, which is implied by basic Markov model. Figure 3 represents the experimental duration distribution and the matched exponential law for the rain and inter-rain event. Clearly a basic Markov model produces a poor approximation for the duration of the events. A Markov model with explicit state duration density [2,4–7] is then adopted for the modelling of the rain and inter-rain duration. An explicit event duration Markov chain enables to model states with every wanted duration distribution.

In the following, the state duration distributions for rain and inter-rain are set to the ones extracted from the experimental rain rate time series. And no attempt to fit them to theoretical distributions is made. The use of an explicit state duration improves the global quality of the model as the duration of the events is more realistic.

2.2. 2nd level: rain rate generation

In fact, rain rate samples are dependent on previous ones [8,9]. The second level of the model takes into account this dependence with NRCD in order to produce valuable rain intensity time series.

The rain rate time series are considered through different intensity intervals such that the observed rain rates are equiprobably spread along them. Every intensity interval defines one state of the Markov chain and the number of intervals is obviously the number of states of the model. Thus, the granularity, i.e., the number of intervals, is adjustable to the level of precision or of simplicity required by the application. In addition, the probability density functions of each state of the Markov model are derived from the experimental rain rate distribution. They correspond to the global rain distribution truncated according to the same intervals.

Figures 4 and 5 deal with a 5-state model example. On Fig. 4 is the sampling of the rain levels to identify the 5 states of the model. Figure 5 is the illustration of the global distribution of rain levels and how it is separated into the different states of the model.

The dynamic behaviour of the second level is defined by the transition probability matrix. The transition matrix is issued from the Next Rain Conditional Distributions from one interval to the other. The NRCDs are quite invariant according to the granularity size, i.e., the number of intervals to be considered. This enforces the hypothesis that the rain rate series are well described by the chosen model. The estimation of the transition vector of state 1 is illustrated on Fig. 6: the NRCD on state 1 (the distribution of rain levels that

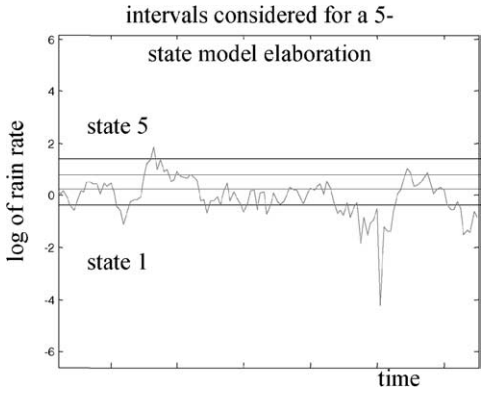

Fig. 4. Separation of rain rate in 5 states.

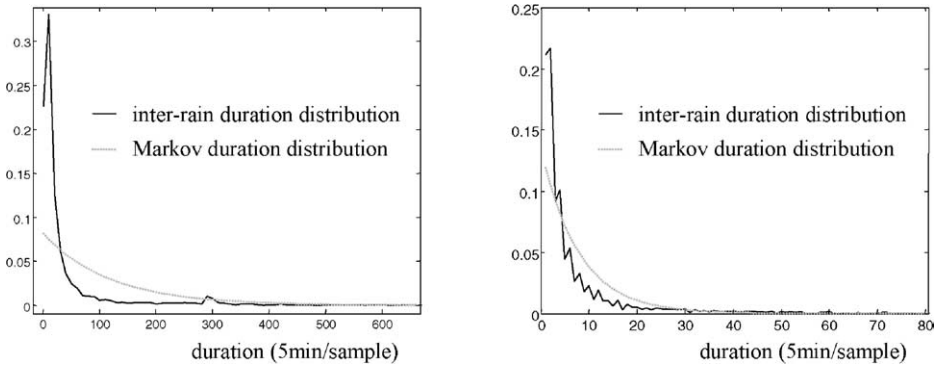

Fig. 3. Experimental duration distribution of rain and inter-rain events and exponential distribution.

immediately follow one rain sample which belongs to state 1), like the global distribution, is truncated. The NRCD is integrated along this partition and the results are the transition probabilities from state 1 to the other states. The same process is applied to every state for the estimation of the complete transition matrix.

The transition matrices for the 20 and 50 state models are also calculated and they are represented on Fig. 7 by a three-dimensional graph. The x and y axis are the number of the considered states, the values of the z axis is the transition probability from state x to state y.

All these transition matrices have been calculated onto data measured in Santiago in Spain. The data are a collection of 10 year observations sampled every 5 min.

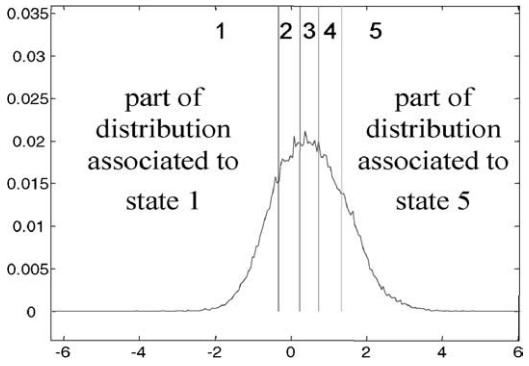

Fig. 5. The distribution of each state is calculated from the global rain rate distribution (right).

At this sampling rate, the transition matrices for the three models (5, 20 and 50 states) show the same characteristics. The main diagonal, which is the probability to remain in the same state, has the highest transition values. The probabilities to evolve from one state to one of its close neighbors are also high whereas the probability to evolve from one state to a very different one is low. This means that physically the rain process is slowly evolving: for example, during a low rain event, there is much more chance for the next rain intensity to be rather small than suddenly very high. The evolution between high and low intensity levels is slow. Moreover, abrupt transitions between low and high intensities can happen (occurrence of a spiky event in a quasi flat one) but are not the most common behavior.

2.3. Model validation

This part presents well known validation tools for assessing the quality of the global two level model. Another tool, a frequentist method, is used. The frequentist method gives an indicator of how well a model matches an observation set. Then this method enables to globally assess the quality of the model whereas the well known validation tools only test the quality of the model on one very particular point.

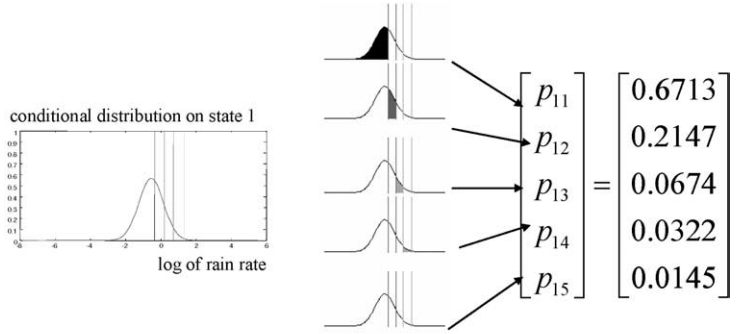

$$\text{complete transition matrix} = \begin{bmatrix} 0.6713 & 0.2147 & 0.0674 & 0.0322 & 0.0145 \\ 0.2355 & 0.4172 & 0.2243 & 0.0876 & 0.0353 \\ 0.0655 & 0.2523 & 0.3791 & 0.2246 & 0.0785 \\ 0.0221 & 0.0899 & 0.2513 & 0.4244 & 0.2124 \\ 0.0056 & 0.0259 & 0.0780 & 0.2312 & 0.6593 \end{bmatrix}$$

Fig. 6. Transition vector and global transition matrix calculated onto conditional distribution on state 1 for a 5 state model example.

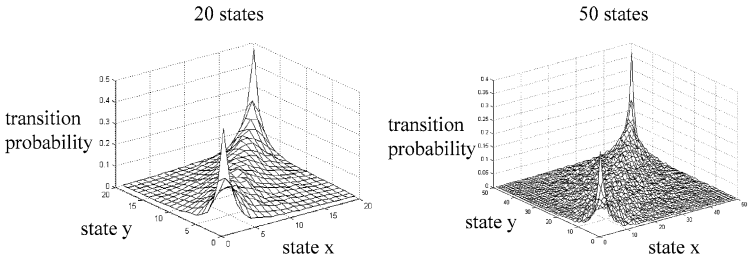

Fig. 7. Transition matrices for the 20 and 50 state models.

Table 1
Comparison between statistics of experimental and simulated data

	experimental	simulated
mean	0.5068	0.5055
variance	0.9353	0.9471
15% lower value	–0.8805	–0.8785
15% upper value	1.96	1.959

2.3.1. *Validation of the models according to statistics*

The inverse cumulative distributions of the log of experimental and simulated rain rate time series are represented on Fig. 8. In Table 1, there are the values for the experimental data and simulated ones for the mean, variance, and 15% upper and lower value. The 15% upper value is the limit value between the 15% highest rain intensities and the others. The second-order statistics [4,10] for four different threshold levels: 1, 2, 5 and 10 mm/h are also presented on Fig. 9. The second order statistic is the probability to have consedutive rain samples higher than R mm/h with the considered rain samples belonging to a single event whose duration $(T_e - T_b)$ is higher than the abscissa. The expression of the second order statistic is $P_R(x, \Delta t) = P(\forall t_0 \in [T_b, T_e], x(t_0) > R$, and $(T_e - T_b) > \Delta t)$ where T_b is the time index of the beginning of the event, T_e of the end. The higher the threshold, the shorter the plots because the probability to encounter a rain event whose every samples are superior to a high threshold diminishes with the duration.

The simulated data match quite accurately the experimental ones. The inverse cumulative distribution of the simulated data is perfectly equal to the experimental data. This perfect matching was expected because of the generation process (part II.B): each state distribution is a representation of a truncation of the rain rate distribution. The data generated by the model in each state are then distributed as a part of the global rain distribution. So, when all these data, belonging to different states, are considered altogether, their distribution is quasi the same as the experimental one. The tested

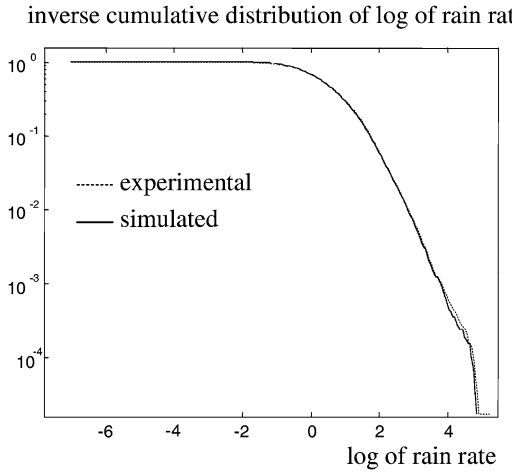

Fig. 8. Inverse cumulative distribution.

model presents also good matching between the experimental and simulated values for the 2nd order statistic: a very small difference between the realized values and the simulated ones is observed. Of course, degradation appears when the threshold R increases but it is mainly due to the low number of events for which all samples are superior to this high threshold.

2.3.2. *Validation of the model according to frequentist method*

In a Bayesian context, different models can be compared using subsequent model probabilities. This strategy only provides performance indicators and does not reveal the true performances of one particular model considering the experimental data. If the model is the correct one, it is straightforward to show (see [11]) that the sequence $\{u_k\}_{k=1\text{K}n}$ with $u_k = P_r(Y_k \leqslant y_k / Y_{0:k-1} = y_{0:k-1}, \theta)$ is a realization of independent identically distributed (i.i.d) variables uniformly distributed on [0, 1] given a realization of the observations $y_{0:n}$ and a model parameter set θ.

The superiority of this validation method on the two previous validation tests is the fact that it judges the global quality and behaviour of the model and not only

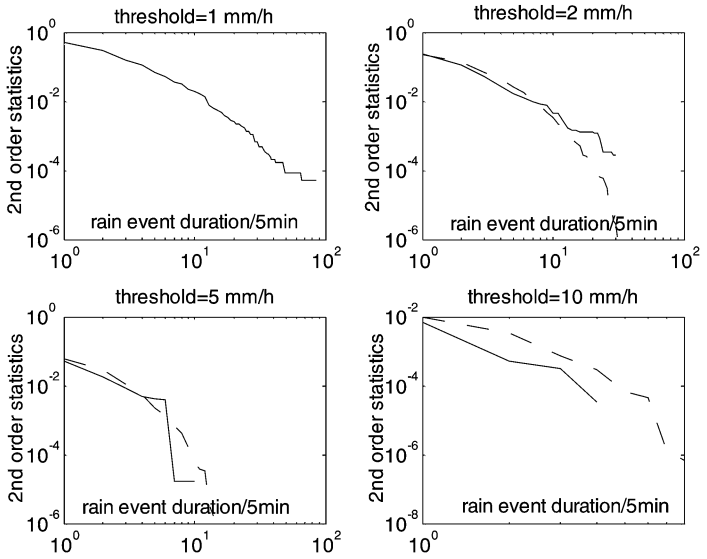

Fig. 9. Second order statistics for four thresholds.

one particular point as the inverse cumulative distribution and the second order statistics do. The inverse cumulative distribution considers the data as a global set in which the order of appearance is not important. So a model can have a perfect inverse cumulative distribution whereas its quality is very poor. The second order statistics is still not investigating every points of the model quality but only how long rain intensities remain above certain threshold values.

Figure 10 is the representation of the distribution of the $\{u_k\}_{k=1...n}$ calculated on the experimental rain rate time series for the 20 and 50-state models. A perfect model would produce a flat histogram equal to the straight line. The $\{u_k\}_{k=1...n}$ have a quite uniform repartition on [0, 1] that means that the quality of the model is good. Further tests on the whiteness and uniform repartition may be performed to attest to the final quality of the proposed model. The state number has high influence on the quality of the model: as expected the model performances are much greater when the number of state is high.

The results presented in Fig. 11 are for the model estimated in Santiago. We also tested the validity of the same 50-state Santiago model for three other locations: Vigo, Lugo, and La Coruña which are towns located around 100 km from Santiago (Fig. 12).

The model estimated in Santiago can not be applied in Vigo or Lugo but it seems that $\{u_k\}_{k=1...n}$ calculated in La Coruña are rather uniform. Further tests, like the comparison of the model obtained in Santiago and in La Coruña, are required but rain characteristics

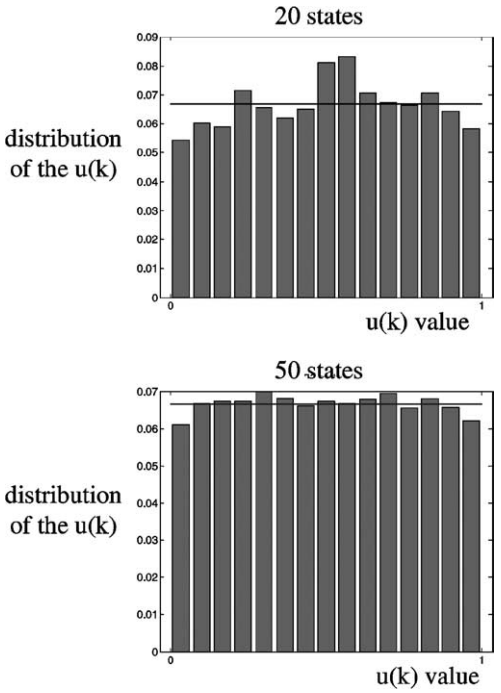

Fig. 10. Distribution of the $\{u_k\}_{k=1\mathrm{K}n}$ for a 20-state model (left) and for a 50-state model (right).

of Santiago and La Coruña appears to be rather similar. This frequentist test may characterise locations presenting same rain characteristics.

In order to compare the frequentist method with more common tests, the rain intensity distributions at the four different locations are compared. The χ^2 dis-

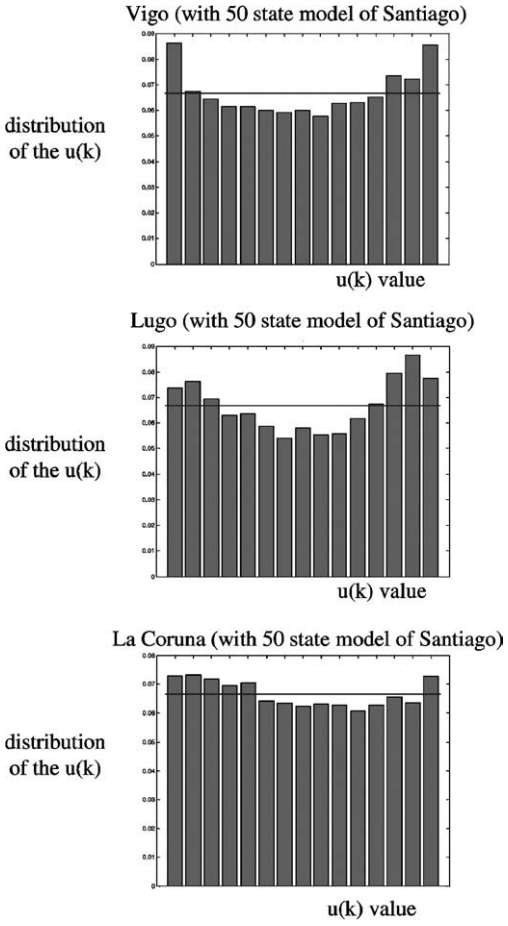

Fig. 11. Quality of the Santiago model applied to Vigo, Lugo and La Coruña rain time series.

tance measures the distance between two probability density functions or distributions. The χ^2 distance between distribution p and reference distribution p_0 is equal for a partition $(c_i)_{1\ldots N}$ of the observation space to:

$$D_{\chi^2}(p_0, p) = \sum_{i=1}^{N} \frac{(p_0(c_i) - p(c_i))^2}{p_0(c_i)}.$$

Table 2 shows the χ^2 distance between the experimental rain cumulative distribution of Santiago and the other location models in the first line. In the second line, there is the distance between the modelled Santiago distribution and the experimental distribution of other locations. The χ^2 results confirm the frequentist ones: Santiago distribution is closer to La Coruña one which means that rain behaviour is more similar in Santiago and in La Coruña. But, contrary to the frequentist method, the χ^2 distance only tells that the two distributions are close and that is not enough to estimate that the model of Santiago can be valid in La Coruña.

Table 2
Distance between Santiago and other location distributions

	Santiago	Lugo	Vigo	La Coruña
χ^2 distance between experimental distributions	0	0.36	0.026	0.018
χ^2 distance between Santiago simulated and experimental distributions	0.0068	0.32	0.032	0.018

If the Santiago model were used to model the rain time series in La Coruña, the second line of Table 2 indicates that the error done on the distribution, 0.018, will be in the same precision range as the error, 0.0068, done by the Santiago model for the simulation of Santiago rain. However, because the error is so large 0.32, as already pointed out the Santiago model can not be used for the generation of Lugo rain time series.

3. Second approach: type model amplitude (TYMA)

The proposed rain rate time-series generator is based on both a signal attenuation time-series generator developed at DLR (Germany) [12] and a single-state generator which was already applied by the authors to the modeling of rain rate time-series [10]. This initial approach included an inter-rain duration distribution, a first-rain distribution and a number of next-rain conditional distributions, $f^{NR}(R_{t+1}|R_t)$, all of them derived from experimental data.

Due to the shortcomings of this single-state model to realistically reproduce both the short- and long-term characteristics of rain rates, an improved four-state model was proposed in [1,6]. The number of states selected was a trade-off between observed differences in rain event characteristics and model complexity. The model in [6] requires 16 state transition probabilities, 4 sets of next-rain distributions and 16 inter-rain duration distributions, all of which were derived form measured data with a clustering algorithm [13,14].

The results obtained with the improved four-state model were reasonably good but, still, further improvements were sought. To achieve this, the measured rain rate time-series were again closely examined, leading

to the identification of embedded short occurrences of strong rates ("spiky" rain) within gently falling rain episodes with small or medium rates. This led the authors to believe that it was more important to model the differences between the "spiky" rain and the gently falling ("quasi-flat") rain occurrences than actually classifying rain events. In order to achieve this, differentiated models had to be developed for the two distinct behaviors.

3.1. Fundamentals of the improved model

In this new version of the model, which can be called two rain type model, a low to medium rate type of rain (quasi-flat rain) is considered to occur in most cases and during most of the time. This rain type corresponds basically to widespread or stratiform rain. For such type of rain, a model similar to the one used in the one- [12] and four-state [6] models is used.

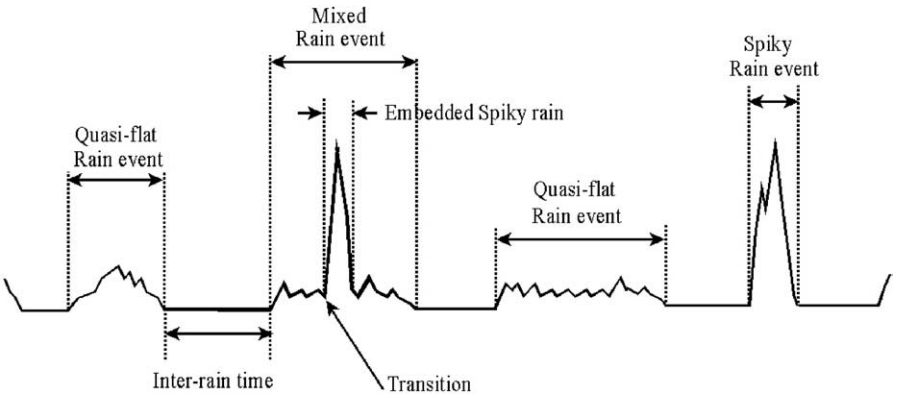

Fig. 12. Quasi-flat, spiky and mixed rain events (two rain type model).

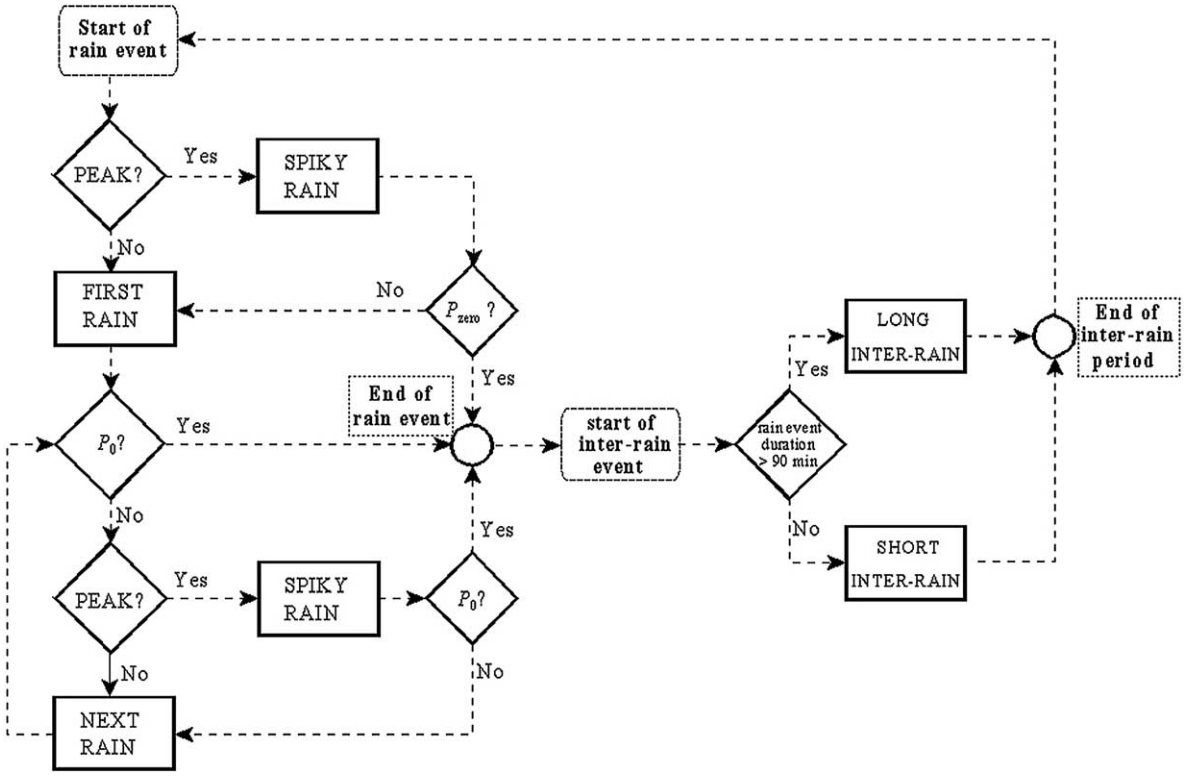

Fig. 13. Two rain type model. Simulator flow diagram.

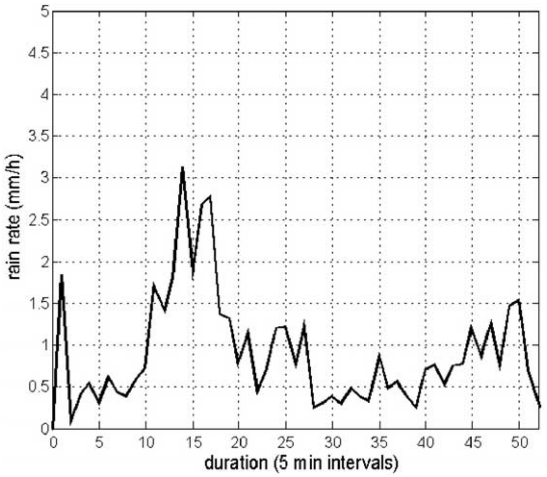

Fig. 14. Example of measured quasi-flat rain rate event.

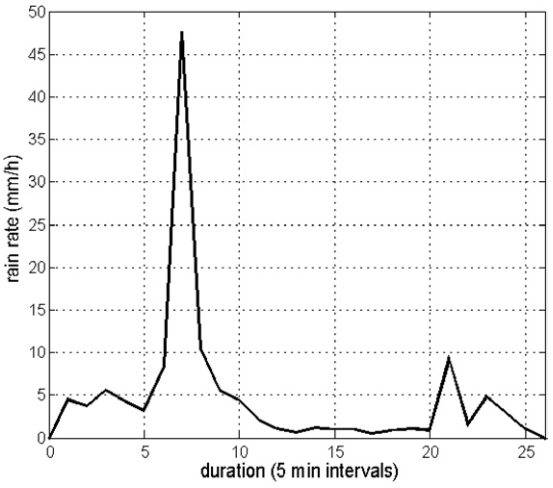

Fig. 15. Example of measured mixed: quasi-flat and spiky rain rate event.

In some cases, spiky, higher rate rain can be observed both forming part of (embedded) quasi-flat rain events, and in stand alone spiky rain events. Spiky rain basically corresponds to local, convective rain. Spiky events are described with a different model to that of quasi-flat events. The threshold between these two types of rain was set at (Rth) 15 mm/h (integration time 5 min) for the analyzed data set. The separation criteria also took into account the slope (*Sp*), which in the case analyzed data was set at 6 mm/h/5 min interval. A simple pattern recognition software was developed to separate out quasi-flat from spiky events, and embedded spiky events within quasi-flat events.

One additional element in the model is the transition probability. This describes the probability of switching from one to the other type of rain. This and other issues relative to the new approach are illustrated with the help of Fig 12. Figure 13 outlines the flow diagram of the model/simulator. The sample spacing may be from 1 to 5 minutes. Higher values, e.g., 10 min, are also possible. This depends very much on the available experimental data.

As indicated above, two sub-models are needed, one for each type of rain. Quasi-flat rain can be modelled by means of conditional distributions as in the single- [12] and four-state [6] models. Thus, Next-Rain Conditional Distributions, NRCDs, $f^{NR}(R_{t+1}|R_t)$, are used. Such NRCDs have been fitted to theoretical distributions, more specifically, to Rayleigh distributions. The fitting has been found to produce a smooth evolution of the parameters for the theoretical distribution except for the first- and the last-rains. This has led to the decision to include in the model a First Rain Distribution, FRD, $f^{FR}(R_{t+1}) = f^{NR}(R_{t+1}|R_t = 0)$. The last rain is discussed later.

The set of NRCD has been fitted with Rayleigh distributions while the FRD has been fitted with a Gamma distribution. Contrary to the four-state case, here only a family of NRCDs is needed (only one state), thus the removal of sub-index i in the notation. This represents an improvement in terms of the number of model parameters that need to be stored.

Even though parameter and distribution fittings have been carried out and those results used in simulations, as shown later, another version of the simulator using measured parameters and distributions (not fitted ones) has been built and results are presented as well.

In the case of spiky rain, the occurrences were very brief, with a typical duration of 10 minutes, i.e., two measured samples, in the case of the rain records used. So far, it has not been possible to fit theoretical distributions to the measured rate and duration distributions. Thus, the measured distribution of rates during spiky events, $f_{\text{Spiky}}(R)$, and the measured distribution of spiky event durations, $f_{\text{Spiky}}(d)$, are used. First, the number of samples is drawn according to the corresponding distribution, and then, the necessary rain intensity samples are generated using $f_{\text{Spiky}}(R)$.

To complete the model, transition probabilities, P_{Peak}, are needed. Probabilities have been extracted both for the case where the rain event starts with a spiky rain or for the case where the spiky rain starts from a quasi-flat rain sample.

Similarly, end of event probabilities, $P_0(d_t)$, have been calculated from measurements. From observations, it has been concluded that these probabilities are

dependent on the duration of the rain event. A single set of $P_0(d_t)$ probabilities has been calculated for the two rain types.

Finally, inter-rain durations can be modelled with an appropriate Inter-Rain Duration Distribution, IRDD, $f^{IR}(d)$. Again, the sub-indices ij have been dropped since only one rainy state is considered. This, again, simplifies significantly the set of parameters required to implement the model. It has been found, however, that two different IRDDs are needed depending on the duration of the preceding rain event. The separation threshold has been found to be of approximately 90 minutes for the analyzed data set. Table 3 summarizes the parameters needed for the new model.

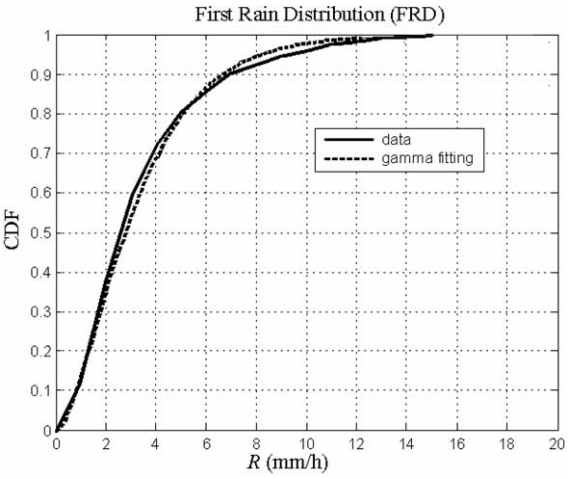

Fig. 16. Cumulative function (measured and fitted) for First Rain.

3.2. Extracted model parameters

In this section the extracted parameters for the model just described are presented for rain rate time-series corresponding to 8 years of recordings of 5 min integrated rain rates taken at Vigo airport in the north-western coast of Spain.

Figure 16 shows the fitting of the measured First-Rain distribution to a Gamma distribution. The fitted parameters are $\alpha = 1.8396$ and $\beta = 1.8241$ where the Gamma pdf is given by the expression

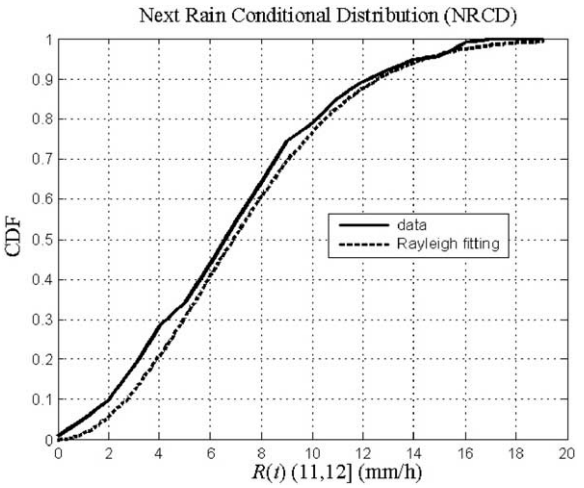

Fig. 17. NRCD for a current rate range in the interval (11,12] (measured and fitted).

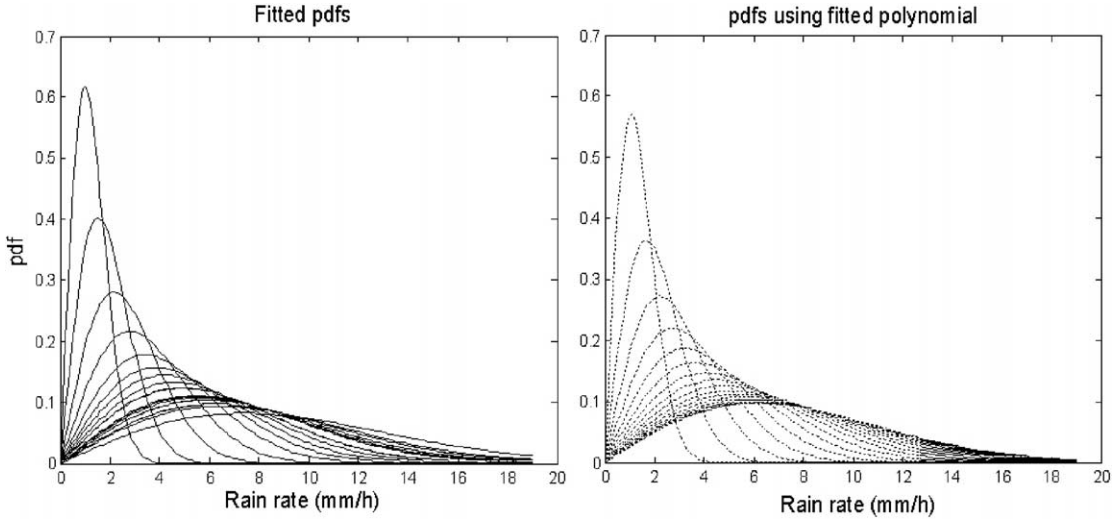

Fig. 18. Family of measured and fitted NRCDs. Left, Rayleigh distributions fitted to actual data. Right, set of Rayleigh distributions from parabolic approximation (Fig. 19).

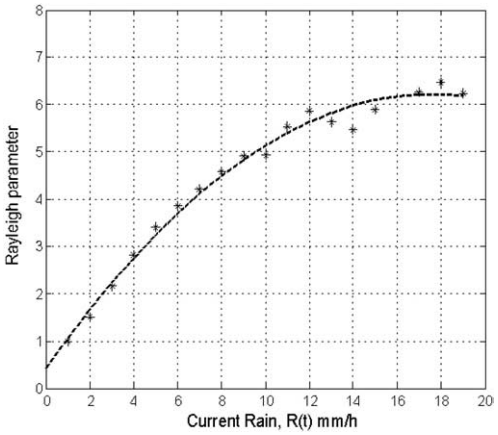

Fig. 19. Curve fitting the evolution of $\sigma(R_t)$.

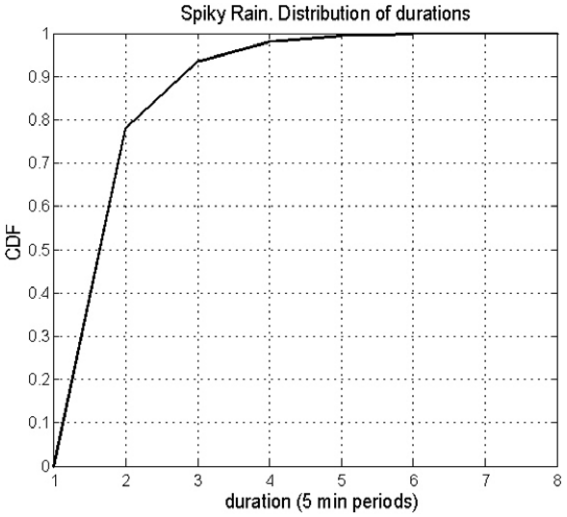

Fig. 20. CDF of durations of spiky events.

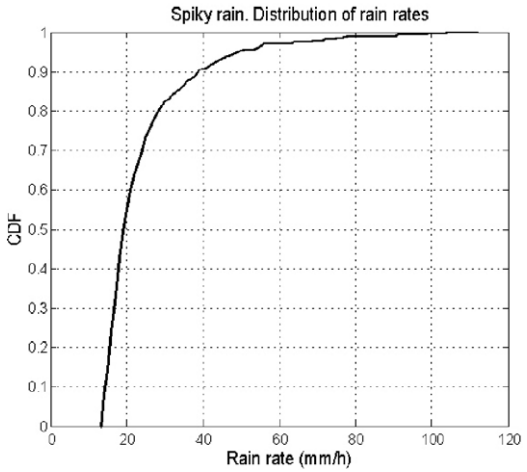

Fig. 21. CDF of rates in spiky events.

Table 3
New model (two rain type) elements

First-Rain distribution	$f^{FR}(R_{t+1})$	Quasi-flat rain
Next-Rain Conditional Distribution, NRCD	$f^{NR}(R_{t+1}\|R_t)$	Quasi-flat rain
Distribution of Spiky rain durations	$f_{\text{Spiky}}(d)$	Spiky rain
Distribution of Spiky rain rates	$f_{\text{Spiky}}(R)$	Spiky rain
End of event distribution	$P_0(d_t)$	Quasi-flat and Spiky rain
Transitions	P_{Peak}	Quasi-flat and Spiky rain
Inter-Rain Duration Distribution, IRDD	$f^{IR}_{\text{Short}}(d)$ and $f^{IR}_{\text{Long}}(d)$	Inter-rain durations: both short and long previous rain event

$$f(x) = \frac{\beta(\beta x)^{\alpha-1}e^{-\beta x}}{\Gamma(\alpha)} \quad x \geqslant 0.$$

Figure 17 shows a fitting example for one member of the family of NRCDs, more specifically, for a current rate range in the interval $R_t = (11, 12]$. Rayleigh distributions have been used in this case, where its pdf is given by

$$f(x) = \frac{x}{\sigma^2}\exp\left(-\frac{x^2}{2\sigma^2}\right) \quad \text{for } x \geqslant 0.$$

The calculated Rayleigh parameters, σ, are listed in Table 4.

Figure 18 shows the family of fitted NRCDs. On Fig. 18-left, the actually fitted distributions are shown. The evolution of the Rayleigh parameter, σ, has also been studied and the following polynomial was fitted (Fig. 19) to describe the evolution of $\sigma(R_t), P(x) = -0.0186x^2 + 0.6557x + 0.4275$.

Taking into account the above polynomial, a new family of NRCDs has been produced which is shown in Fig. 18-right.

The above parameters are used to model the quasi-flat rain type. For the spiky rain two parameters are needed, the distribution of intensities, $f_{\text{Spiky}}(R)$, and the distribution event durations, $f_{\text{Spiky}}(d)$. It has not

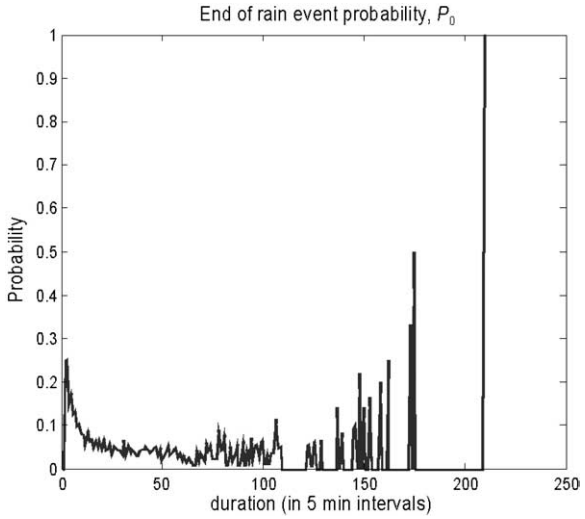

Fig. 22. Extracted values of P_0 for different current rains R_t.

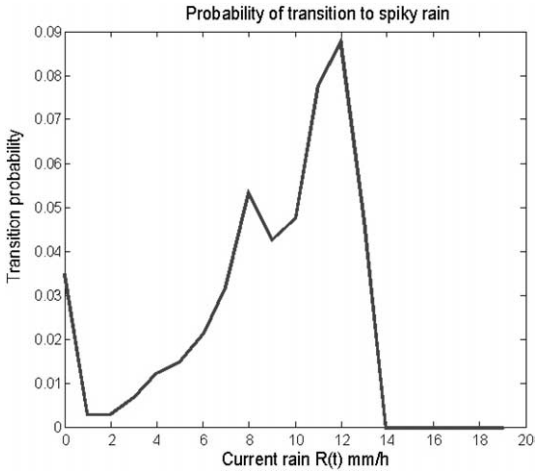

Fig. 23. Extracted transition probabilities, P_{Peak}, from different current rain levels to spiky rain.

been possible to find a theoretical distribution that fits those measured distributions. Thus, it has been decided to use the measured distributions shown in Figs 20 and 21 in the simulations.

Finally, Fig. 22 shows the extracted P_0 values for different current rains, R_t, Fig. 23 shows the extracted transition probabilities from null rain rate or from quasi-flat rain rates to spiky rain, and Fig. 24 illustrates the two inter-rain event duration distributions, for after long ($\geqslant$90 min) rain events and short ($<$90 min) rain events.

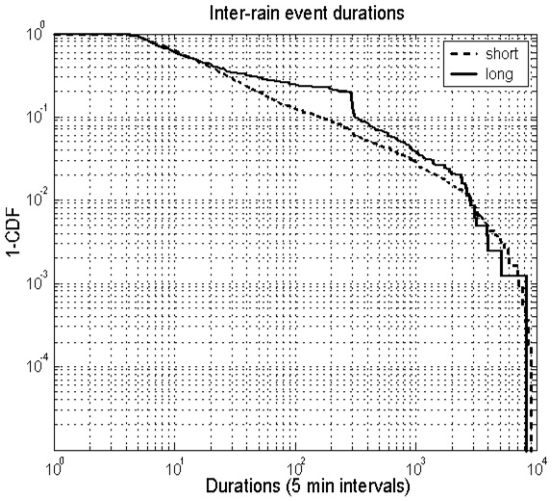

Fig. 24. Inter-rain event duration distributions. After long ($\geqslant$90 min) and short ($<$90 min) rain events.

Table 4
Evolution of $\sigma(R_t)$

R_t	$\sigma(R_t)$	R_t	$\sigma(R_t)$
		(9,10]	4.9268
(0,1]	0.9832	(10,11]	5.5311
(1,2]	1.5068	(11,12]	5.8579
(2,3]	2.1607	(12,13]	5.6373
(3,4]	2.8090	(13,14]	5.4639
(4,5]	3.4144	(14,15]	5.8745
(5,6]	3.8519	(15,16]	7.3784
(6,7]	4.2058	(16,17]	6.2607
(7,8]	4.5816	(17,18]	6.4785
(8,9]	4.9054	(18,19]	6.2386

3.3. Model tests

To test the model, long simulations covering periods of several years have been run. The simulated time-series have been compared with the measured ones in the following terms:

1. The overall cumulative distribution.
2. Second order statistics of rain rates for different rates: $R = 0, 1, 5, 10, 20$ mm/h.
3. Inter-rain event duration distribution.

Two versions of the model have been implemented, namely, one using measured distributions and other using fitted distributions. Slightly better matches have been achieved with the first implementation. Figures 25–28 show the comparisons mentioned above. First-order statistics can be reproduced quite accurately. As for the second-order statistics, good agree-

ment has been achieved for some of the thresholds considered. However, there is still room for further improvement.

4. Further work and conclusions

This paper presents two rain-rate time-series generators that match, with a good degree of approximation, the first- and second-order statistics of measured rain rates recorded in the northwest of Spain. In addition to these commonly used statistics for validation, we also resort to new validation tools based on a frequentist method.

Despite some differences between them, the two models present major similarities. Both models are hierarchic Markov chain; their first level models the alternation of "rain" and "no-rain"; they both use the experimental distributions to determine the duration of any rain or inter-rain events. But, contrary to the EMMA approach, which only differentiates rain and inter-rain events, the second model isolates four different cases: quasi-flat rain event, spiky rain events, inter-rain following a long rain event, and inter-rain following a short rain event. As a result, the first approach requires the extraction of two duration distributions and the second one, four.

The second levels of both models are directly concerned by the generation of rain intensities. EMMA model is very simple to use and to derive with adjustable granularity. It considers the whole rain data and use the NRCDs and the global rain distribution to

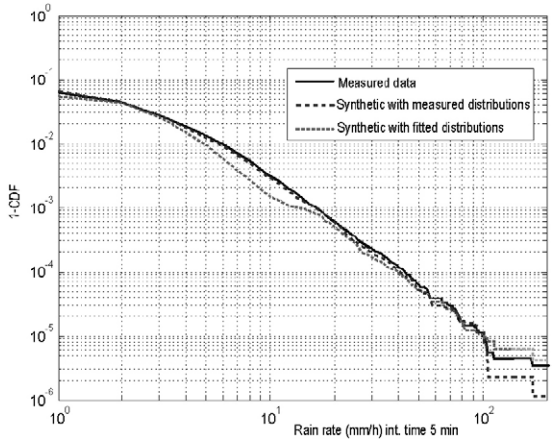

Fig. 25. Inverse cumulative distribution. Overall simulated and measured time-series.

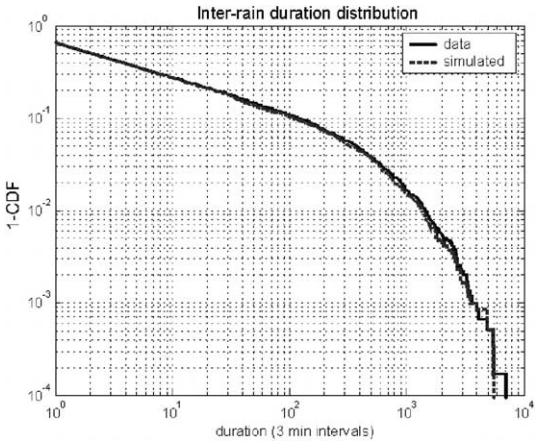

Fig. 26. Inverse CDF of measured and simulated inter-rain event durations.

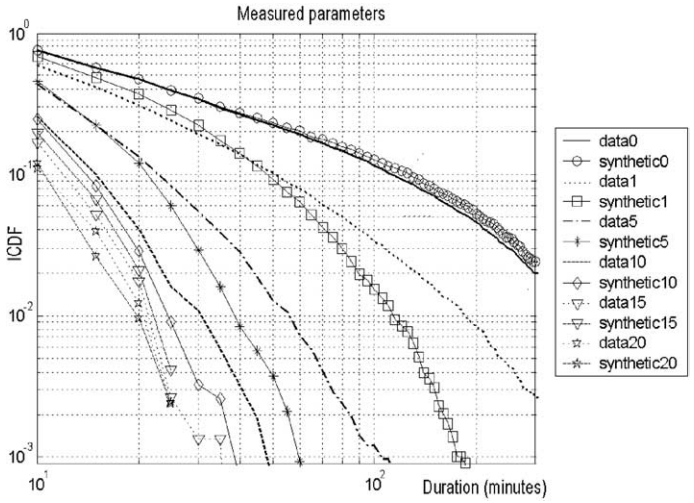

Fig. 27. Inverse CDF of durations of events exceeding several thresholds in mm/h using the simulator version with measured distributions.

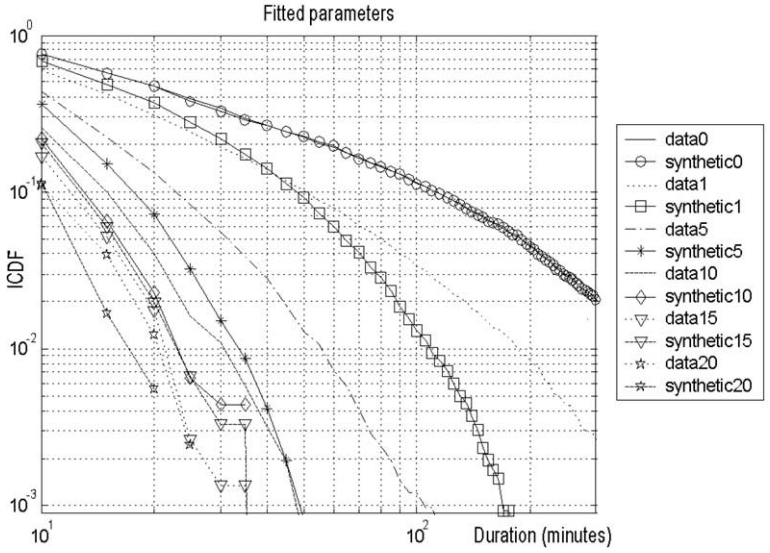

Fig. 28. Inverse CDF of durations of events exceeding several thresholds in mm/h using the simulator version with fitted distributions.

extract the parameters of itsexplicit Markov chain. The TYMA approach is more sophisticated: first it identifies two a priori types of rain behaviour: spiky and quasi flat events. It also takes into account the distribution of the first samples for quasi-flat rain events. In the same way as the first model, it also uses the NRCDs for the generation of the quasi-flat rain events as the first model.

There are numerous similarities between the two approaches presented in this paper. As a major observation, the TYMA model reflects more physical phenomena, needs more parameters and is more complex. Both approaches are shown to simulate high quality time series. Besides, further tests and comparison will be required to determine the exact advantages of each one on performance results.

The aim is to reach a trade-off between simplicity and accuracy so the derived model can be extended to other climatic areas by simply changing the input parameter set. In view of the fact that rain rates and signal attenuation are highly correlated, further objectives are to exploit the widespread availability of recorded rain information from different climatic areas. This will allows us to fill in the incomplete statistics of regions where signal attenuation data are unavailable. In addition, the two-level model share great similarities with the Onera N-state model [2,3] for rain attenuation time series. This reinforces the hypothesis that rain attenuation and rain rates are strongly correlated.

Acknowledgements

The rain rate database used in this study was supplied by the Radiocommunications Group at the Polytechnic University of Madrid. This work has been partially funded by the CICYT of Spanish Ministry of Science and Technology (TIC2001-3701-C02-01/02) and the Regional Government of Galicia (Spain), Xunta de Galicia (PGIDT01TIC30301PR). DLR has funded a 2 month stage of A.Nuñez at its Wessling site. Part of this work has been carried out in the framework of European research programs COST 280 and SatNEx.

References

[1] F. Pérez-Fontan, U.-C. Fiebig, C. Enjamio, L. Husson and A. Benarroch, Synthetic rain-rate time-series generation for radio system Simulation, in: *ClimDiff*, 2003.

[2] L. Castanet, T. Deloues and J. Lemorton, Channel modelling based on N-state Markov chains for satcom system simulation, in: *ICAP 2003*, Exeter, UK, 2003.

[3] L. Castanet, T. Deloues and J. Lemorton, Methodology to simulate long-term propagation time series from the identification of attenuation periods filled with synthesized events, in: *COST 272-280 International Workshop on Satellite Communications from Fade Mitigation to Service Provision*, Noordwijk, The Netherlands, 2003.

[4] F. Pérez-Fontan, U.-C. Fiebig, C. Enjamio, L. Husson and A.I. Castro, Improving rain rate time-series generation for system simulation applications, in: *5th MCM*, 2003.

[5] C. Alasseur, L. Husson and F.P. Fontan, Simulation of rain events time series with Markov model, in: *PIRMC 2004*, Barcelona, Spain, 2004.

[6] U.-C. Fiebig, F. Pérez-Fontán and C. Enjamio, 4-State synthetic rain-rate time-series generator, in: *9th Ka and Broadband Communications Conference*, 2003.

[7] L.E. Bråten and T. Tjelta, Semi-Markov multistate modeling of the land mobile propagation channel for geostationary satellites, *IEEE Trans. on Antennas and Propagation* **50**(12) (2002), 1795–1802.

[8] U.-C. Fiebig, A time-series generator modelling rain fading and its seasonal and diurnal variations, in: *1st International Workshop of COST-Action 280*, Malvern, UK, 2002.

[9] M.M.J.L. van de Kamp, Rain attenuation as a Markov process: the meaning of two samples, in: *COST 280, 1st International Workshop*, 2002.

[10] U.C. Fiebig and F.P. Fontan, First results on modeling rain rates, in: *4th COST 280 Meeting*, Prague, Czech Republic, 2002.

[11] M. Rosenblatt, Remarks on a multivariate transformation, *Ann. Math. Statist.* **23** (1952), 447–472.

[12] U.C. Fiebig, Modelling rain fading with a time-series generator considering seasonal and diurnal variations, in: *Proc. 8th Ka-Band Utilization Conference*, Baveno, Italy, 2002.

[13] Y. Wong and E.C. Posner, A new clustering algorithm applicable to multispectral and polarimetric SAR Images, *IEEE Trans. on Geoscience and Remote Sensing* **31**(3) (1993).

[14] L. Husson. J.C. Dany, K. Berradi, S. Chambon and A. Beffani, Scalable multi-state Markovian modeling of time series of received power from measurements of mobile satellite transmissions in the L-band, in: *IEEE VTC '02*, Spring, 2002.